

Brief Report

Characterization of Red Sea Bream (*Pagrus major*) Interferon Regulatory Factor 5 and 6 Genes and Their Expression in Response to RSIV Infection

Kyung-Ho Kim ^{1,†}, Min-Soo Joo ^{1,2,†}, Gyoungsik Kang ¹, Won-Sik Woo ¹, Min-Young Sohn ¹, Ha-Jeong Son ¹ and Chan-Il Park ^{1,*}

¹ Department of Marine Biology and Aquaculture, College of Marine Science, Gyeongsang National University, 2, Tongyeonghaean-ro, Tongyeong 53064, Republic of Korea

² East Sea Fisheries Research Institute, National Institute of Fisheries Science, Gangneung-si 25435, Republic of Korea

* Correspondence: parkci@gnu.ac.kr

† These authors contributed equally to this work.

Abstract: Interferon regulatory factors (IRFs) play crucial roles in antiviral processes, such as in the transcriptional induction of interferon (IFN) and IFN-stimulated genes (ISGs). In this study, the genes encoding IRF5 and IRF6 were identified in *Pagrus major*, and their expression in various organs after pathogen infection was analyzed. In the coding sequences of *P. major* (*Pm*)IRF5 and *Pm*IRF6, the DNA binding domain, IRF association domain, and viral-activated domain were found to be highly conserved. Phylogenetic analysis revealed that *Pm*IRF5 and *Pm*IRF6 were most closely related to IRF5 and IRF6 of large yellow croakers. The mRNAs for *Pm*IRF5 and *Pm*IRF6 were constitutively expressed in all organs analyzed but were highly expressed in the liver and gills. As a result of an infection with red sea bream iridovirus, a major pathogen of red sea bream, *Pm*IRF5 and *Pm*IRF6 expression was significantly upregulated in the spleen and kidney. On the basis of these results, it can be concluded that IRF5 and IRF6 expression play an influential role in the immune system of red sea bream infected with viruses.

Keywords: red sea bream; red sea bream iridovirus; interferon regulatory factors; expression analysis



Citation: Kim, K.-H.; Joo, M.-S.; Kang, G.; Woo, W.-S.; Sohn, M.-Y.; Son, H.-J.; Park, C.-I. Characterization of Red Sea Bream (*Pagrus major*) Interferon Regulatory Factor 5 and 6 Genes and Their Expression in Response to RSIV Infection. *Fishes* **2023**, *8*, 114. <https://doi.org/10.3390/fishes8020114>

Academic Editor: Eric Hallerman

Received: 25 January 2023

Revised: 14 February 2023

Accepted: 15 February 2023

Published: 16 February 2023



Copyright: © 2023 by the authors. Licensee MDPI, Basel, Switzerland. This article is an open access article distributed under the terms and conditions of the Creative Commons Attribution (CC BY) license (<https://creativecommons.org/licenses/by/4.0/>).

1. Introduction

Interferon regulatory factors (IRFs) are essential regulators involved in the transcriptional induction of interferon (IFN) and IFN-stimulated genes (ISGs) [1]. In addition, IRFs are critical components of innate and adaptive immunity, playing significant roles in antiviral defense, immune response, cell growth regulation, and apoptosis [2,3]. Currently, 11 IRF families (IRF1–11) have been identified in vertebrates, with IRF10 in birds and IRF11 in fish [1,3–6]. The N-terminus of IRF contains a DNA binding domain (DBD) of approximately 120 amino acids (aa), containing 5–6 conserved tryptophan repeats forming a helix-turn-helix motif [7]. It recognizes and binds IFN-stimulated response elements (ISREs) to regulate the expression of several immune-related genes [8–10]. IRFs contain an IRF association domain (IAD) at their non-conserved C-terminus, which mediates the interaction of IRFs with other transcription factors to form transcriptional complexes [7,11,12]. IRFs are classified into three groups based on differences in the C-terminal region. The IRF family members are activators (IRF1, 3, 5, 7, 9, and 10), repressors (IRF2 and 8), and multifunctional factors that inhibit and activate gene transcription (IRF2, 4, 5, and 7) [4,6,13,14].

Mammalian IRF5 regulates the expression of IFN- α and IFN- β to participate in antiviral responses, activate inflammatory factors, and suppress tumors [15–17]. It has been shown that IRF5 knockout mice show high susceptibility to viral infections and are involved in the TLR-MyD88 signaling pathway for gene induction of proinflammatory cytokines,

such as interleukin (IL)-6, IL-12, and TNF α [16,18,19]. Mammalian IRF6 is associated with the formation of connective tissue, and mutations in the IRF6 gene can cause Van der Woude syndrome (VWS) and popliteal pterygium syndrome (PPS); however, it has been reported that it is not related to IFN expression [20–22]. The overexpression of fish IRF6 significantly upregulated IFN promoter activity and activated the transcription of ISG15, RIG-I, and MAVS [23]. In addition, IRF6 can be phosphorylated by MyD88 and TBK1 and is an IFN-positive regulator, in contrast to mammalian IRF6 [23]. Nevertheless, reports of them in teleost fish are extremely rare, except for zebrafish (*Danio rerio*), half-smooth tongue sole (*Cynoglossus semilaevis*), mandarin fish (*Siniperca chuatsi*), Atlantic cod (*Gadus morhua*), and blunt snout bream (*Megalobrama amblycephala*) [23–28]. Identifying IRF5 and IRF6 in fish models and studying their functional characteristics will assist in predicting the prognosis of related diseases. This will enable us to understand their roles in the immune system.

Red sea bream iridovirus (RSIV) is a DNA virus that causes mortality in more than 30 species of farmed fish. The first report on RSIV was made in 1990 on red sea bream (*Pagrus major*) cultured in Japan [29,30]. Since it was first reported in 1998 in aquaculture rock bream (*Oplegnathus fasciatus*), RSIV has led to significant economic losses in the Republic of Korea yearly [31]. To reduce the damage caused by RSIV, basic research, disease prevention, and control measures must be prepared. Although these efforts have continued over time, there is still limited information regarding the immune system in particular. Therefore, in this study, the first nucleotide sequences of *IRF5* and *IRF6* identified in red sea bream were obtained, and their characteristics were confirmed. In addition, by confirming the expression patterns of *P. major* (*Pm*)*IRF5* and *PmIRF6* mRNA after RSIV exposure, we intend to provide new insights into IRF5 and IRF6 in the red sea bream immune system.

2. Materials and Methods

2.1. Experimental Fish

Red sea bream were obtained from a net pen farm in Tongyeong (Gyeongsangnam-do, Republic of Korea) and used in the experiment. To ensure that the fish were not infected with pathogens, five randomly selected fish were tested in the laboratory for bacterial, parasitic, and viral diseases. The first step was to observe the external symptoms of the fish with a microscope and with the naked eye. This was to ensure that they were not infected with parasites. During the procedure, the spleen and kidney were removed, and tissue cuts were smeared on the brain and heart infusion agar medium to determine if bacteria were present. RSIV infection was confirmed using DNA extraction from the spleen and PCR using primers recommended by WOA and qPCR in the references. The purpose of this was to confirm the virus was not infected [30,32]. Red sea bream (total length: 12.5 ± 1.6 cm, weight: 52.1 ± 4.6 g) were acclimatized in a 1600 L tank for 2 weeks before the experiment and filtered. In addition, UV-treated seawater was continuously flowing. During the acclimatization period, the water temperature was 22 ± 1 °C, and commercial feed was fed twice daily.

2.2. Virus

In August 2019, the spleen of RSIV-infected rock bream was collected, and the tissue sample was stored at -80 °C [33]. WOA provided a sequencing method through PCR that confirmed the presence of RSIV [30]. RSIV was classified as RSIV genotype II (accession number: AY532608) by phylogenetic analysis of major capsid protein gene sequences [34].

Before the infection experiment, RSIV-infected tissue was homogenized in phosphate-buffered saline (PBS) and centrifuged at $10,000 \times g$ for 20 min at 4 °C. After filtering the supernatant containing the virus with a 0.45 μ m syringe filter, it was inoculated into a *P. major* fin (PMF) cell line [35]. The PMF cell line was provided by the National Fishery Products Quality Management Service (Busan, Republic of Korea) and was cultured at 25 °C in L-15 medium (Gibco) and supplemented with 10% fetal bovine serum (FBS) (Gibco), 1% antibiotic-antimycotic (A-A; 100 U/mL penicillin, 100 μ g/mL streptomycin,

and 25 µg/mL amphotericin B, Gibco). PMF cells were then inoculated with filtered RSIV. After 4 h of infection, the medium was replaced with an L-15 medium containing 10% FBS and 1% A-A and cultured for 7 d. The cell supernatant containing the virus was used as an inoculum for subsequent experiments to observe the expression patterns of *PmIRF5* and *PmIRF6* mRNA in RSIV-challenged red sea bream.

2.3. Sequence and Phylogenetic Analysis of *PmIRF5* and *PmIRF6* Genes

The coding sequences (CDSs) of *PmIRF5* and *PmIRF6* were obtained through the RNA-seq method of next-generation sequencing (NGS) analysis using RNA extracted from the RSIV-stimulated spleen of red sea bream. Sanger sequencing was performed to verify the complete length sequence of the CDS, and PCR was conducted with the primer set shown in Table 1. *IRF5* and *IRF6* nucleotide sequences and deduced amino acid sequence analysis were performed with the GENETYX program version 8.0 (Genetyx Corporation, Tokyo, Japan) and the Basic Local Alignment Search Tool (BLAST) algorithm of the National Center for Biotechnology Information (NCBI). Molecular weight and isoelectric point (pI) were predicted using the Expert Protein Analysis System ProtParam tool (ExPASy) (<http://web.expasy.org/protparam/> (accessed on 1 July 2020)). To identify specific domains and motifs of *PmIRF5* and *PmIRF6*, the Simple Modular Architecture Research Tool (SMART) (<http://smart.embl-heidelberg.de/> (accessed on 2 October 2020)) and SignalP version 6.0 software (<https://services.healthtech.dtu.dk/service.php?SignalP-6.0> (accessed on 7 November 2022)) were analyzed. Multiple sequence alignments to amino acid sequences from different fish species were analyzed with Clustal Omega (<https://www.ebi.ac.uk/Tools/msa/clustalo/> (accessed on 1 February 2022)). The phylogenetic analysis was conducted using the neighbor-joining (NJ) method of the MEGA (Molecular Evolutionary Genetics Analysis) version X program, and bootstraps were repeated 2000 times.

Table 1. Primer sequences used in this study.

Primer Name	Sequence of Primer (5'–3')	Usage
<i>PmIRF5</i> -F1	ATGAGCGTGCAGCCTCGGA	Amplification for reaffirmation of full-length CDS
<i>PmIRF5</i> -R1	TGTCCCTCCGGTGGACAGAC	
<i>PmIRF5</i> -F2	AGGGACATTTGGACCTCCTC	
<i>PmIRF5</i> -R2	TGTAGAACCGCTGCTTCTGG	
<i>PmIRF5</i> -F3	GCGTTTCTACACTGAGGCC	
<i>PmIRF5</i> -R3	TCAGGGGACATTGGGGGTCC	
<i>PmIRF6</i> -F1	ATGTCAGTCAACCCTCGGC	
<i>PmIRF6</i> -R1	CTCTTTGGGCCAGACCTCGT	
<i>PmIRF6</i> -F2	TCAGACTCCTCCATGCAGCC	
<i>PmIRF6</i> -R2	TGGGCTATCACCCACTGAG	
<i>PmIRF6</i> -F3	TTTTCTCAGTGGGGTGATAG	
<i>PmIRF6</i> -R3	TCACTGTCCCTGCATAAC	
qPCR- <i>PmIRF5</i> -F	ACCTGTTTGGACCTGTCACC	
qPCR- <i>PmIRF5</i> -R	AGCAGGGCCTCAGTGTAGAA	
qPCR- <i>PmIRF6</i> -F	CTCTGCCAGTGCAAGGTGTA	
qPCR- <i>PmIRF6</i> -R	GGCTATCACCCACTGAGAA	
qPCR- <i>PmEF-1α</i> -F	ACGTGTCCGTCAAGGAAATC	
qPCR- <i>PmEF-1α</i> -R	TGATGACCTGAGCGTTGAAG	
qPCR-RSIV-Meg 1041-F	CCACCAGATGGGAGTAGAC	RSIV copy number determination [32]
qPCR-RSIV-Meg 1139-R	GGTTGATATTGCCCATGTCCA	
qPCR-RSIV-Meg 1079-P	[FAM]CCTACTA[i-EBQ]CTTTGCGCCAGCATG[phosphate]	

2.4. Viral Challenge, Nucleic Acid Extraction, and cDNA Synthesis

To confirm the distribution of the mRNA expressions of *PmIRF5* and *PmIRF6* from healthy red sea bream, head and trunk kidneys, skin, stomach, gills, heart, liver, spleen, eyes, brain, and intestines of three fish were aseptically collected and stored at −80 °C.

To observe the mRNA expression patterns of *PmIRF5* and *PmIRF6* in various organs of red sea bream after being infected with RSIV, 100 µL of RSIV inoculum (1×10^7 RSIV copies/fish) was artificially injected intraperitoneally in a 500 L water tank at 25 °C. At 0 (control, no infection), 1, 3, 6, 12, 24, and 36 h and 3, 5, and 7 d after virus inoculation, the gills, spleen, liver, and trunk kidneys were aseptically removed from three fish. Total RNA extraction from collected tissues was performed using the easy-spin Total RNA Extraction Kit (iNtRON Biotechnology, Seongnam, Republic of Korea) according to the manufacturer's manual. cDNA synthesis was performed using the PrimeScript 1st strand cDNA Synthesis Kit (Takara, Kusatsu, Japan). Further, 8 µL of total RNA, 1 µL of the random hexamer, and 1 µL of dNTP mixture were heated at 65 °C for 5 min and then cooled on ice for 5 min. Then, 4 µL of 5× PrimeScript buffer, 0.5 µL of RNase Inhibitor (40 U/µL), 1 µL of PrimeScript RTase (200 U/µL), and 4.5 µL of RNase-free water were added and mixed carefully. A reaction mixture of 20 µL was heated at 30 °C for 10 min and 42 °C for 1 h. Subsequently, the reaction was heated at 95 °C for 5 min to inactivate the enzyme, and the synthesized cDNA was stored at −20 °C pending use. Genomic DNA extraction was performed using the AccuPrep Genomic DNA Extraction Kit (Bioneer, Daejeon, Republic of Korea) according to the manufacturer's manual. All experimental protocols followed the guidelines of the Institutional Animal Care and Use Committee of Gyeongsang National University (approval number: GNU-220427-E0041).

2.5. Quantitative PCR Analysis

An RSIV copy number determination was performed according to a previously reported method [32]. The final volume of the reaction mixture was 25 µL and consisted of 12.5 µL of the HS Prime qPCR Premix with UDG (2×) (Genetbio, Daejeon, Republic of Korea), 900 nM of each primer, 250 nM of the probe, and 5 µL of DNA. There were 45 cycles of 5 s at 95 °C followed by 10 s at 60 °C, with one cycle lasting 1 min at 95 °C.

A reverse transcription quantitative PCR (RT-qPCR) was performed to measure the mRNA expression levels for *PmIRF5* and *PmIRF6* using the SYBR green method. The RT-qPCR reaction mixture consisted of 12.5 µL TB Green premix Ex Taq (Takara), 400 nM of each primer, and 1 µL cDNA in a final volume of 25 µL. The RT-qPCR reaction conditions were initial denaturation at 95 °C for 10 min, followed by denaturation at 95 °C for 20 s, and annealing at 60 °C for 1 min for a total of 45 cycles. Final dissociation was performed at 95 °C for 15 s, then at 60 °C for 30 s, and lastly at 95 °C for 15 s. Melt curve analysis was performed at the end of the 45 amplification cycles to test for the presence of the unique PCR products.

The relative expression levels of *PmIRF5* and *PmIRF6* mRNA were compared with the threshold cycle (Ct) of the mRNA of the elongation factor 1 alpha gene (*EF-1α*; GenBank accession No. AY190693), known as a red sea bream housekeeping gene, and quantified using the $2^{-\Delta\Delta Ct}$ method, ($\Delta\Delta Ct = 2^{-[\Delta Ct_{\text{sample}} - \Delta Ct_{\text{internal control}}]}$) [36]. The experiment was performed in triplicate. The PCR reaction was analyzed using Thermal Cycler Dice Real-Time System III (Takara), and the sequences of primer sets and probes used are shown in Table 1.

2.6. Statistical Analysis

The expression analysis of *PmIRF5* and *PmIRF6* in organs during RSIV infection was assessed using a one-way analysis of variance (ANOVA), followed by Tukey's multiple comparison tests (* $p < 0.05$ and ** $p < 0.01$) and compared to controls (0 h). The statistical analysis was performed using GraphPad Prism 9.5.

3. Results

3.1. Identification and Characterization of *PmIRF5* and *PmIRF6* Sequence

The CDSs of *PmIRF5* and *PmIRF6* are 1455 bp (GenBank accession No. OK340058) and 1479 bp (GenBank accession No. OK340059), respectively (Figure S1). The CDS of *PmIRF5* encodes a mature peptide of 484 aa with a calculated molecular weight of 54.5 kDa and an

isoelectric point of 5.11 (Figure S1A). The CDS of *PmIRF6* encodes a 492 aa peptide with a molecular weight of 55.5 kDa and an isoelectric point of 5.12 (Figure S1B). *PmIRF5* was confirmed to have a DBD (3–116 aa) with five tryptophan (W) residues at the N-terminus, IAD (253–436 aa), a viral activated domain (VAD; 436–472 aa) at the C-terminus, and two nuclear localization signals (NLSs; 5–11 aa, 413–419 aa) (Figure S1A). In addition, *PmIRF6* contained a DBD (3–116 aa) with five W residues at the N-terminus, IAD (246–430 aa), and VAD (430–468 aa) at the C-terminus (Figure S1B). As a result of the multiple sequence alignment, *PmIRF5* had the highest similarity with large yellow croaker *IRF5* (89.84%), followed by rock bream *IRF5* (88.8%), turbot *IRF5* (82.62%), Japanese flounder *IRF5* (80.16%), and Atlantic salmon *IRF5* (77.35%). There was a comparatively low level of identity with channel catfish *IRF5* (68.11%), zebrafish *IRF5* (63.39%), and Mississippi paddlefish *IRF5* (61.2%) (Figure 1A). In *PmIRF6*, mi-uy croaker *IRF6* (93.5%) showed the highest similarity, followed by large yellow croaker *IRF6* (93.29%), Atlantic salmon *IRF6* (78.59%), grass carp *IRF6* (76.11%), and zebrafish *IRF6* (71.63%) (Figure 1B). As a result of phylogenetic analysis using the deduced amino acid sequences, *PmIRF5* and *PmIRF6* were clustered into corresponding subgroups and showed the closest relationship to marine fish. In addition, *IRF5* and *IRF6* in marine fish, freshwater fish, and mammals each formed distinct clusters (Figure 2).



Figure 1. Multiple sequence alignment analysis of the (A) *IRF5*- and (B) *IRF6*-derived amino acid sequences in various fish species. Red double-headed arrows at the N-termini indicate the DNA binding domain (DBD), with five conserved tryptophan residues indicated by black arrows. The blue double-headed arrows at the C-termini indicate the IRF association domain (IAD), while the viral-activated domain (VAD) is indicated by the yellow double-headed arrows. The nuclear localization signals (NLSs) are indicated by green double-headed arrows.

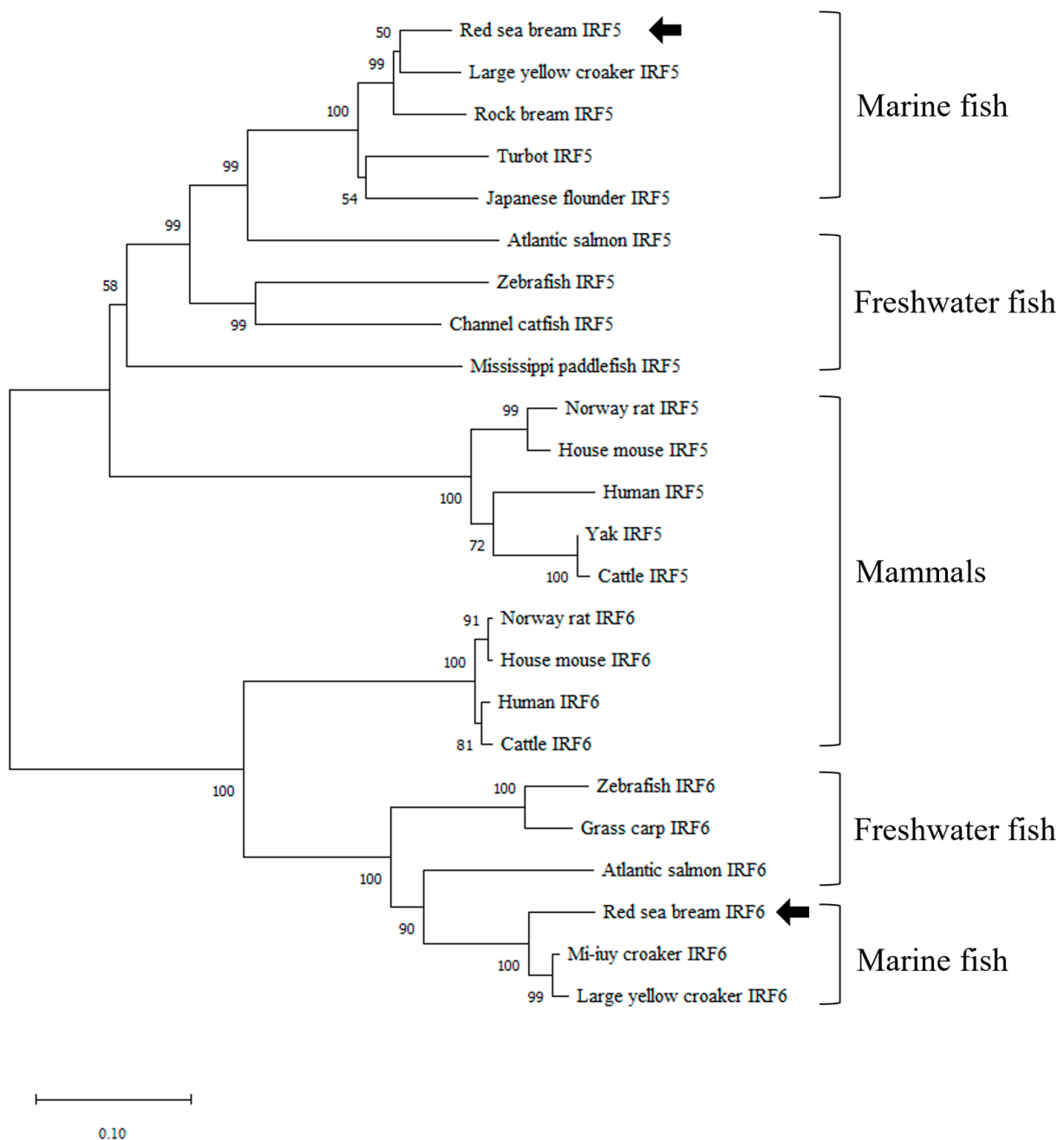


Figure 2. A phylogenetic tree of *P. major* interferon regulatory factor (*PmIRF5*), *PmIRF6*, and other known *IRF5* and *IRF6* homologs based on the neighbor-joining (NJ) method. The scale bar indicates a branch length of 0.10. Numbers are bootstrap percentiles from 2000 replicates. This analysis is based on the following sequence data: Red sea bream *IRF5* (UIR15468), Large yellow croaker *IRF5* (QPZ85366), Rock bream *IRF5* (AFZ93894), Turbot *IRF5* (AEG76960), Japanese flounder *IRF5* (AEY55357), Atlantic salmon *IRF5* (NP_001133324), Channel catfish *IRF5* (AHH37262), Zebrafish *IRF5* (NP_001314746), Mississippi paddlefish *IRF5* (AEW27153), Norway rat *IRF5* (NP_001100056), House mouse *IRF5* (EDL13770), Human *IRF5* (EAL24108), Yak *IRF5* (ELR49399), Cattle *IRF5* (NP_001030542), Norway rat *IRF6* (NP_001102329), House mouse *IRF6* (NP_058547), Human *IRF6* (AAH14852), Cattle *IRF6* (NP_001070402), Grass carp *IRF6* (AMT92196), Zebrafish *IRF6* (NP_956892), Atlantic salmon *IRF6* (XP_014022332), Red sea bream *IRF6* (UIR15469), Large yellow croaker *IRF6* (QPZ85367), and Mi-iuy croaker *IRF6* (AHB59739).

3.2. Expression of *PmIRF5* and *PmIRF6* mRNA in Various Organs

As a result of analyzing the distribution of *PmIRF5* and *PmIRF6* mRNA in various organs of healthy red sea bream, they were ubiquitously expressed in all 11 organs (head and trunk kidneys, skin, stomach, gills, heart, liver, spleen, eyes, brain, and intestine) (Figure 3). In comparison to the stomach where *PmIRF5* mRNA was least expressed, the liver demonstrated the highest expression (7.52-fold), followed by the brain (7.24-fold) and eyes (7.12-fold). The expression level was relatively low in the intestine (1.83-fold), heart (1.93-fold), and trunk kidneys (2.21-fold) (Figure 3A). As compared to the heart, *PmIRF6* mRNA expression was highest in the gills (252.75-fold), and moderately high levels were found in the intestine (85.0-fold) and liver (77.56-fold). A relatively low level of expression was observed in the spleen (2.81-fold), the brain (5.39-fold), and the head kidneys (7.68-fold) (Figure 3B).

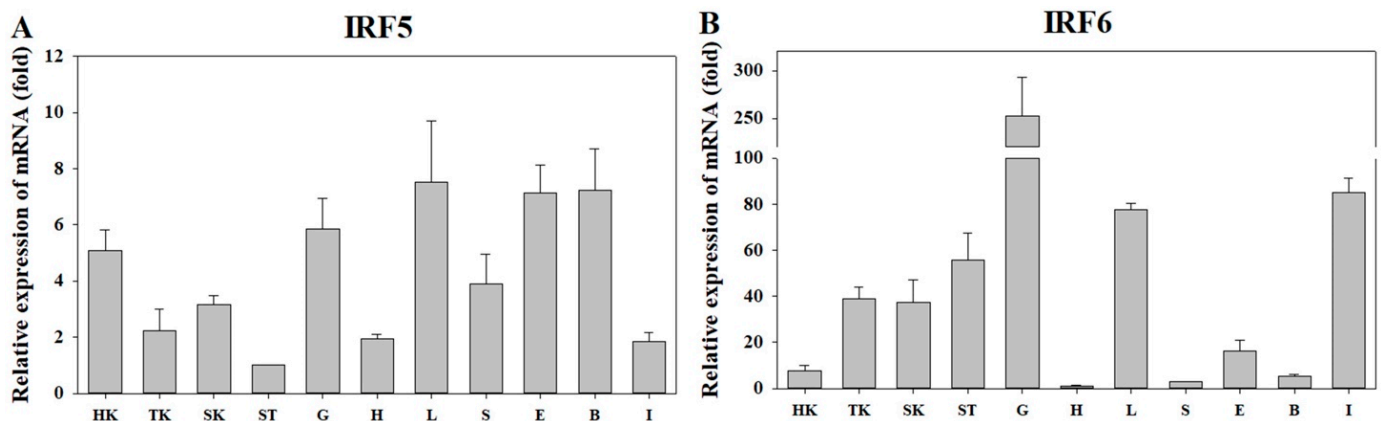


Figure 3. Distribution of (A) *IRF5* and (B) *IRF6* mRNA expression related to *EF-1 α* expression in red sea bream organs (exhibited relative to the organ with the lowest mRNA expression level). The 11 organs are the head kidneys (HK), trunk kidneys (TK), skin (SK), stomach (ST), gills (G), liver (L), heart (H), spleen (S), eyes (E), brain (B), and intestine (I). Results exhibit the mean \pm SD of triplicate ($n = 3$).

3.3. Expression of *PmIRF5* and *PmIRF6* mRNA after RSIV Challenge

The mRNA expression levels of *PmIRF5* and *PmIRF6* in the gill, spleen, liver, and kidney at 0, 1, 3, 6, 12, 24, and 36 hpi (hours post-infection) and 3, 5, and 7 dpi (days post-infection) after RSIV infection were determined using RT-qPCR. The expression of *PmIRF5* mRNA was mostly upregulated in all tested organs, and limited downregulated was observed (Figure 4A). The expression was significantly upregulated at 1 and 6 hpi in the gill and 1, 6, 12, 24 hpi, and 5 dpi in the spleen. In the kidney, the expression value was significantly increased at 3, 6, 24, and 36 hpi. In contrast, significant downregulation was confirmed in the gills and liver at 7 dpi. The highest expression level was observed at 6 hpi in the kidney (5.73-fold) (Figure 4A). As a result of RSIV exposure, *PmIRF6* mRNA exposure was mostly upregulated in all organs tested, and some organs showed a decrease in expression. The expression value in the gills decreased significantly at 3 hpi, upregulated at 6 hpi, and downregulated again at 12 hpi. In addition, there was significant upregulation of expression in the spleen at 6 and 24 hpi. Furthermore, a significant increase in expression was observed at 3 hpi and from 3 to 5 dpi in the liver, and at 1 hpi and from 36 hpi to 5 dpi in the kidney (Figure 4B).

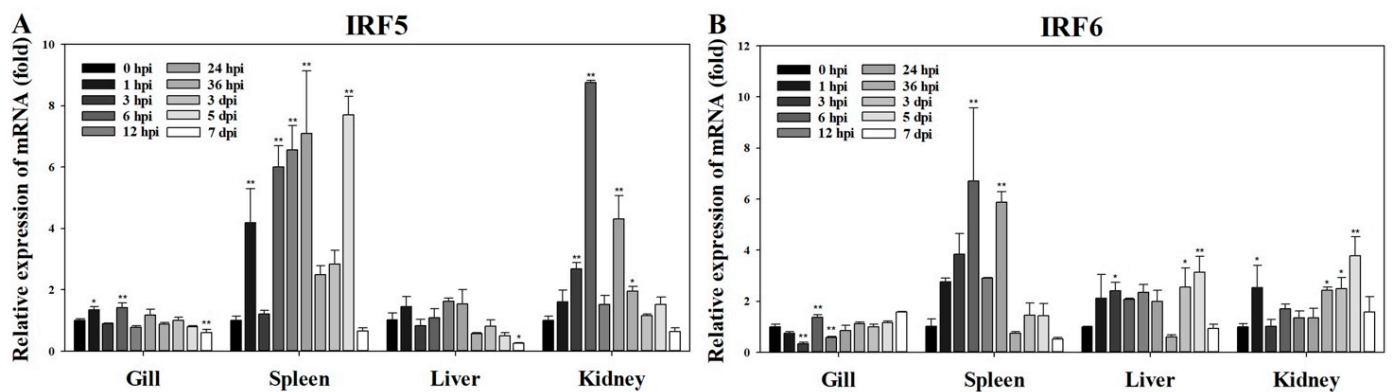


Figure 4. Expression pattern of (A) *IRF5* and (B) *IRF6* mRNA in the gill, spleen, liver, and kidney of red sea bream infected with RSIV. The *PmIRF5* and *PmIRF6* transcription levels were compared to that of the *EF-1 α* using RT-qPCR. The data are shown as the means \pm SD of triplicate for each organ ($n = 3$). Asterisks indicate differences (* $p < 0.05$, ** $p < 0.01$) compared with the control (0 h).

4. Discussion

The IRF family of transcription factors plays an essential role in regulating type I IFNs and ISGs [8]. The *IRF5* and *IRF6* genes have been identified in several vertebrates. Despite this, there is no information on the identification of *IRF5* and *IRF6* in red sea bream and their expression patterns following infection with RSIV, a severe viral disease. In this study, we identified the full-length CDSs of *PmIRF5* and *PmIRF6*. As with other fish species, *IRF5* and *IRF6* encode conserved W residues, DBD, IAD, and VAD. The DBDs of *PmIRF5* and *PmIRF6* contain five well-conserved W pentad-repeats that form a helix-turn-helix structure that binds to the ISRE/IRF regulatory element (IRF-E) consensus in target promoters via contacts [37,38], as do other vertebrates with *IRF5* and *IRF6*. The five W residues of both *PmIRF5* and *PmIRF6* were located at 13, 28, 40, 60, and 79 aa, which compares to those of *IRF5* in zebrafish [39], grass carp [40], and turbot [41] and those of *IRF6* in common carp [42] and zebrafish [24]. Among these, three W residues have been reported to be involved in binding to DNA through hydrogen bonding by recognizing the “GAAA” sequence [38]. A further feature of the C-terminus of *PmIRF5* and *PmIRF6* is the presence of IAD1, which is similar to those of *IRF3–9*. In the IRF family, IADs consist of IAD1 (*IRF3–9*) and IAD2 (*IRF1* and 2), which are structurally different [3,43]. IADs can initiate the transcription of target genes by forming transcriptional complexes with other IRFs or transcriptional co-regulators [44,45]. The VAD contains conserved serine residues in other vertebrate IRFs that are phosphorylation sites during viral infection. These functions are similar to those of the serine-rich domains (SRDs) of *IRF3* and *IRF7* [46,47]. The VAD domain is greatly involved in the transcriptional activity of *IRF7* in response to viral infection, with its deletion resulting in transcriptionally inactive *IRF7* [48]. Additionally, the deletion of only the C-terminal SRD results in no virus-induced transcriptional activity, suggesting that the VAD domain alone is not transcriptionally active and requires cooperation with the SRD to play its important role in the antiviral response. Similarly to other *IRF5*s, the predicted *PmIRF5* protein contains two NLSs at its N- and C-termini, and these NLSs are vital for IRF nuclear translocation and maintenance in virus-infected cells [2]. NLSs were identified in *IRF1*, 3, 4, 5, 8, and 9, of which only *IRF5* contained two NLSs, with the others containing one in the N-terminal domain [2]. Previous studies reported that the N-terminal NLS and C-terminal NLS of *IRF5* are involved in nuclear translocation, with the N-terminal NLS playing a more significant role [2]. Overall, these generally conserved amino acid sequences and structural features of *PmIRF5* and *PmIRF6* suggest that their activation and action patterns in the immune response to viral infection have remained relatively unchanged.

Phylogenetic analysis indicated that all *IRF5* and *IRF6* family members were divided into marine fish, freshwater fish, and mammalian groups. In addition, *PmIRF5* and *PmIRF6*

were more closely related to large yellow croaker *IRF5* and *6*, including *IRF5* and *6* of marine fish. These results are consistent with the observed evolutionary relationship between the various tibia species at the genomic and structural level of the *IRF5* and *6* genes.

PmIRF5 and *PmIRF6* mRNAs were ubiquitously expressed in all organs examined. In particular, *PmIRF5* was expressed at high levels in the liver, brain, eyes, and gills, and high levels of *PmIRF6* were found in the gills, intestines, and liver. Similarly, rock bream *IRF5* was highly expressed in the liver [49], and common carp *IRF5* was highly expressed in the gills and brain [50]. It was found that *IRF6* was highly expressed in the gills, liver, and intestines of large yellow croakers, which is consistent with our findings [51]. The high expression of *IRF5* and *IRF6* in the gills and intestine, and mucosal-associated lymphoid tissues with lymphocytes, suggests that they may play a significant role in the activity of the mucosal immune system in fish.

IRF5 and *IRF6* mRNA expression was significantly upregulated in RSIV-infected red sea bream, particularly in the spleen and kidneys which are important target organs of the virus [30,32] and may, therefore, require higher levels of immunity than other organs. In contrast, *IRF5* and *IRF6* mRNAs were highly expressed in the gills of healthy red sea bream. This may be explained by the constantly exposure of the teleost fish to potential pathogens present in the aquatic environment [52]. In addition, the relatively low immunity in the gills of the infected fish may have been due to the delivery of RSIV antigen via the peritoneal cavity. Further studies on the effect of the infection method on the expression patterns of antiviral genes in different organs are required. Turbot significantly stimulated the expression of *IRF5* in the spleen on 1 dpi and the kidney on 2 dpi after infection with turbot reddish body iridovirus (TRBIV) [41]. After infection with rock bream iridovirus (RBIV), *IRF5* expression in the head kidney was greatest at 12 hpi and decreased until 48 hpi [49]. Nevertheless, in a time course study of grass carp infected with grass carp hemorrhagic reovirus (GCRV), high upregulation of *IRF5* (>300-fold) was observed in the head kidney at 6 d after infection [40]. Among Japanese flounders infected with the Lymphocystis disease virus (LCDV), significant upregulation was observed in the muscle at 3 dpi [53]. Considering that *IRF5* mediates the antiviral response in a virus-specific manner, further research on the expression pattern of *IRF5* according to the host-virus relationship is necessary. Atlantic cod showed no significant changes in *IRF6* expression in response to poly(I:C) and lipopolysaccharide stimulation [27]. While these results are consistent with the understanding that *IRF6* plays an instrumental role in epithelial cell differentiation, a previous study showed evidence of an upregulation of *IRF6* following poly(I:C) stimulation [23]. Currently, limited information is available on the expression profile of *IRF6* in fish following exposure to pathogens. During our study, we found that *IRF6* levels were upregulated after RSIV stimulation in red sea bream and that distinct changes were observed in the spleen in particular. However, information regarding the functional characterization of *IRF6* by pathogen infection in fish is still limited, and further research is required. *IRF5* and *IRF6* are known to stimulate the expression of IFN-related genes in virus-infected cells [15–17,23]. Our results showed that the expression of *PmIRF5* and *PmIRF6* mRNA was low in all organs at 7 dpi. Red sea bream infected with RSIV showed onset of death at 6 dpi and 100% cumulative mortality at 8 dpi. Therefore, at this time, RSIV infection may have disrupted host cell function, or apoptosis may have disrupted the transcription of immune genes.

In summary, we identified and characterized the CDSs of the *IRF5* and *IRF6* genes in red sea bream. *PmIRF5* and *PmIRF6* appeared to be constitutively expressed in several organs, such as the liver and gills of red sea bream. Red sea bream infected with RSIV showed upregulation of *PmIRF5* and *PmIRF6* in the spleen and kidney at an early stage of infection. Functional studies of *IRF5* and *IRF6* on viral diseases in teleost fish are still limited. Furthermore, developing an understanding of pathogen-derived diseases and the immune system will be essential for the effective control and treatment of disease.

5. Conclusions

We identified the genetic sequences of *PmIRF5* and *PmIRF6* in red sea bream and characterized their corresponding aa sequences and conserved domains. Analysis of the Expression profiles of *PmIRF5* and *PmIRF6* mRNAs revealed that they are constitutively expressed and that, post-infection, they significantly increase in the spleen and kidneys, which are major targets of RSIV.

Supplementary Materials: The following supporting information can be downloaded at: <https://www.mdpi.com/article/10.3390/fishes8020114/s1>, Figure S1: (A) *PmIRF5* and (B) *PmIRF6* nucleotide sequence and translated amino acid sequence. The red box at the N-terminus indicates the DNA binding domain (DBD), and five conserved tryptophan residues are marked with arrows. The blue box at the C-terminus indicates the IRF association domain (IAD), and the viral-activated domain (VAD) is shown in the yellow box. The nuclear localization signals (NLS) are shown in green boxes.

Author Contributions: Conceptualization, K.-H.K., M.-S.J. and C.-I.P.; methodology, K.-H.K. and M.-S.J.; formal analysis, K.-H.K., G.K., W.-S.W., M.-Y.S. and H.-J.S.; investigation, K.-H.K.; resources, C.-I.P.; writing—original draft preparation, K.-H.K.; writing—review and editing, C.-I.P.; supervision, C.-I.P.; project administration, C.-I.P.; funding acquisition, C.-I.P. All authors have read and agreed to the published version of the manuscript.

Funding: This research was funded by the Ministry of Oceans and Fisheries, Republic of Korea (R2023024).

Institutional Review Board Statement: All experimental protocols followed the guidelines of the Institutional Animal Care and Use Committee of the Gyeongsang National University (approval number: GNU-220427-E0041).

Data Availability Statement: Not applicable.

Acknowledgments: This research was supported by the National Institute of Fisheries Science, Ministry of Oceans and Fisheries, Republic of Korea (R2023024).

Conflicts of Interest: The authors declare no conflict of interest.

References

1. Honda, K.; Taniguchi, T. IRFs: Master regulators of signaling by toll-like receptors and cytosolic pattern-recognition receptors. *Nat. Rev. Immunol.* **2006**, *6*, 644–658. [[CrossRef](#)] [[PubMed](#)]
2. Barnes, B.J.; Kellum, M.J.; Field, A.E.; Pitha, P.M. Multiple regulatory domains of IRF-5 control activation, cellular localization, and induction of chemokines that mediate recruitment of T lymphocytes. *Mol. Cell. Biol.* **2002**, *22*, 5721–5740. [[CrossRef](#)]
3. Yanai, H.; Negishi, H.; Taniguchi, T. The IRF family of transcription factors: Inception, impact and implications in oncogenesis. *Oncoimmunology* **2012**, *1*, 1376–1386. [[CrossRef](#)]
4. Nehyba, J.; Hrdlicková, R.; Burnside, J.; Bose, H.R., Jr. A novel interferon regulatory factor (IRF), IRF-10, has a unique role in immune defense and is induced by the v-Rel oncoprotein. *Mol. Cell. Biol.* **2002**, *22*, 3942–3957. [[CrossRef](#)] [[PubMed](#)]
5. Huang, W.S.; Zhu, M.H.; Chen, S.; Wang, Z.X.; Liang, Y.; Huang, B.; Nie, P. Molecular cloning and expression analysis of a fish specific interferon regulatory factor, IRF11, in orange spotted grouper, *Epinephelus coioides*. *Fish Shellfish Immunol.* **2017**, *60*, 368–379. [[CrossRef](#)]
6. Huang, B.; Qi, Z.T.; Xu, Z.; Nie, P. Global characterization of interferon regulatory factor (IRF) genes in vertebrates: Glimpse of the diversification in evolution. *BMC Immunol.* **2010**, *11*, 22. [[CrossRef](#)] [[PubMed](#)]
7. Tamura, T.; Yanai, H.; Savitsky, D.; Taniguchi, T. The IRF family transcription factors in immunity and oncogenesis. *Annu. Rev. Immunol.* **2008**, *26*, 535–584. [[CrossRef](#)]
8. Taniguchi, T.; Ogasawara, K.; Takaoka, A.; Tanaka, N. IRF family of transcription factors as regulators of host defense. *Annu. Rev. Immunol.* **2001**, *19*, 623–655. [[CrossRef](#)]
9. Veals, S.A.; Schindler, C.; Leonard, D.; Fu, X.Y.; Aebersold, R.; Darnell, J.E.; Levy, D.E. Subunit of an alpha-interferon-responsive transcription factor is related to interferon regulatory factor and Myb families of DNA-binding proteins. *Mol. Cell. Biol.* **1992**, *12*, 3315–3324. [[CrossRef](#)]
10. Darnell, J.E., Jr.; Kerr, I.M.; Stark, G.R. Jak-STAT pathways and transcriptional activation in response to IFNs and other extracellular signaling proteins. *Science* **1994**, *264*, 1415–1421. [[CrossRef](#)]
11. Panne, D.; Maniatis, T.; Harrison, S.C. An atomic model of the interferon-beta enhanceosome. *Cell* **2007**, *129*, 1111–1123. [[CrossRef](#)] [[PubMed](#)]

12. Chen, W.; Royer, W.E., Jr. Structural insights into interferon regulatory factor activation. *Cell. Signal.* **2010**, *22*, 883–887. [[CrossRef](#)] [[PubMed](#)]
13. Antonczyk, A.; Krist, B.; Sajek, M.; Michalska, A.; Piaszyk-Borychowska, A.; Plens-Galaska, M.; Wesoly, J.; Bluysen, H.A.R. Direct inhibition of IRF-dependent transcriptional regulatory mechanisms associated with disease. *Front. Immunol.* **2019**, *10*, 1176. [[CrossRef](#)] [[PubMed](#)]
14. Hu, G.; Chen, X.; Gong, Q.; Liu, Q.; Zhang, S.; Dong, X. Structural and expression studies of interferon regulatory factor 8 in Japanese flounder, *Paralichthys olivaceus*. *Fish Shellfish Immunol.* **2013**, *35*, 1016–1024. [[CrossRef](#)]
15. Schoenemeyer, A.; Barnes, B.J.; Mancl, M.E.; Latz, E.; Goutagny, N.; Pitha, P.M.; Fitzgerald, K.A.; Golenbock, D.T. The interferon regulatory factor, IRF5, is a central mediator of toll-like receptor 7 signaling. *J. Biol. Chem.* **2005**, *280*, 17005–17012. [[CrossRef](#)]
16. Krogsgaard, M.; Li, Q.J.; Sumen, C.; Huppa, J.B.; Huse, M.; Davis, M.M. Agonist/endogenous peptide-MHC heterodimers drive T cell activation and sensitivity. *Nature* **2005**, *434*, 238–243. [[CrossRef](#)]
17. Hu, G.; Mancl, M.E.; Barnes, B.J. Signaling through IFN regulatory factor-5 sensitizes p53-deficient tumors to DNA damage-induced apoptosis and cell death. *Cancer Res.* **2005**, *65*, 7403–7412. [[CrossRef](#)]
18. Takaoka, A.; Yanai, H.; Kondo, S.; Duncan, G.; Negishi, H.; Mizutani, T.; Kano, S.; Honda, K.; Ohba, Y.; Mak, T.W.; et al. Integral role of IRF-5 in the gene induction programme activated by toll-like receptors. *Nature* **2005**, *434*, 243–249. [[CrossRef](#)]
19. Paun, A.; Reinert, J.T.; Jiang, Z.; Medin, C.; Balkhi, M.Y.; Fitzgerald, K.A.; Pitha, P.M. Functional characterization of murine interferon regulatory factor 5 (IRF-5) and its role in the innate antiviral response. *J. Biol. Chem.* **2008**, *283*, 14295–14308. [[CrossRef](#)]
20. Ingraham, C.R.; Kinoshita, A.; Kondo, S.; Yang, B.; Sajan, S.; Trout, K.J.; Malik, M.I.; Dunnwald, M.; Goudy, S.L.; Lovett, M.; et al. Abnormal skin, limb and craniofacial morphogenesis in mice deficient for interferon regulatory factor 6 (Irf6). *Nat. Genet.* **2006**, *38*, 1335–1340. [[CrossRef](#)]
21. Richardson, R.J.; Dixon, J.; Malhotra, S.; Hardman, M.J.; Knowles, L.; Boot-Handford, R.P.; Shore, P.; Whitmarsh, A.; Dixon, M.J. Irf6 is a key determinant of the keratinocyte proliferation-differentiation switch. *Nat. Genet.* **2006**, *38*, 1329–1334. [[CrossRef](#)] [[PubMed](#)]
22. Leslie, E.J.; Standley, J.; Compton, J.; Bale, S.; Schutte, B.C.; Murray, J.C. Comparative analysis of IRF6 variants in families with Van der Woude syndrome and popliteal pterygium syndrome using public whole-exome databases. *Genet. Med.* **2013**, *15*, 338–344. [[CrossRef](#)] [[PubMed](#)]
23. Li, S.; Lu, L.F.; Wang, Z.X.; Chen, D.D.; Zhang, Y.A. Fish IRF6 is a positive regulator of IFN expression and involved in both of the MyD88 and TBK1 pathways. *Fish Shellfish Immunol.* **2016**, *57*, 262–268. [[CrossRef](#)] [[PubMed](#)]
24. Ben, J.; Jabs, E.W.; Chong, S.S. Genomic, cDNA and embryonic expression analysis of zebrafish IRF6, the gene mutated in the human oral clefting disorders van der Woude and popliteal pterygium syndromes. *Gene Expr. Patterns* **2005**, *5*, 629–638. [[CrossRef](#)]
25. Zhang, J.; Li, Y.X.; Hu, Y.H. Molecular characterization and expression analysis of eleven interferon regulatory factors in half-smooth tongue sole, *Cynoglossus semilaevis*. *Fish Shellfish Immunol.* **2015**, *44*, 272–282. [[CrossRef](#)]
26. Laghari, Z.A.; Li, L.; Chen, S.N.; Huo, H.J.; Huang, B.; Zhou, Y.; Nie, P. Composition and transcription of all interferon regulatory factors (IRFs), IRF1–11 in a perciform fish, the mandarin fish, *Siniperca chuatsi*. *Dev. Comp. Immunol.* **2018**, *81*, 127–140. [[CrossRef](#)]
27. Inkpen, S.M.; Solbakken, M.H.; Jentoft, S.; Eslamloo, K.; Rise, M.L. Full characterization and transcript expression profiling of the interferon regulatory factor (IRF) gene family in Atlantic cod (*Gadus morhua*). *Dev. Comp. Immunol.* **2019**, *98*, 166–180. [[CrossRef](#)]
28. Zhan, F.B.; Jakovlić, I.; Wang, W.M. Identification, characterization and expression in response to *Aeromonas hydrophila* challenge of five interferon regulatory factors in *Megalobrama amblycephala*. *Fish Shellfish Immunol.* **2019**, *86*, 204–212. [[CrossRef](#)]
29. Inouye, K.; Yamano, K.; Maeno, Y.; Nakajima, K.; Matsuoka, M.; Wada, Y.; Sorimachi, M. Iridovirus infection of cultured red sea bream, *Pagrus major*. *Fish Pathol.* **1992**, *27*, 19–27. [[CrossRef](#)]
30. WOAHA (World Organisation for Animal Health). Red Sea bream iridoviral disease. In *Manual of Diagnostic Tests for Aquatic Animals*; WOAHA: Paris, France, 2012; Available online: https://www.woaah.org/fileadmin/Home/eng/Health_standards/aahm/current/2.3.07_RSIVD.pdf (accessed on 29 March 2022).
31. Sohn, S.G.; Choi, D.L.; Do, J.W.; Hwang, J.Y.; Park, J.W. Mass mortalities of cultured striped beakperch, *Oplegnathus fasciatus* by iridovirus infection. *Fish Pathol.* **2000**, *13*, 121–127.
32. Kim, K.H.; Choi, K.M.; Kang, G.; Woo, W.S.; Sohn, M.Y.; Son, H.J.; Yun, D.; Kim, D.H.; Park, C.I. Development and validation of a quantitative polymerase chain reaction assay for the detection of red sea bream Iridovirus. *Fishes* **2022**, *7*, 236. [[CrossRef](#)]
33. Kim, K.H.; Choi, K.M.; Joo, M.S.; Kang, G.; Woo, W.S.; Sohn, M.Y.; Son, H.J.; Kwon, M.G.; Kim, J.O.; Kim, D.H.; et al. Red sea bream Iridovirus (RSIV) kinetics in rock bream (*Oplegnathus fasciatus*) at various fish-rearing seawater temperatures. *Animals* **2022**, *12*, 1978. [[CrossRef](#)]
34. Kim, K.L.; Hwang, S.D.; Cho, M.Y.; Jung, S.H.; Kim, Y.C.; Jeong, H.D. A natural infection by the red sea bream Iridovirus-type Megalocytivirus in the golden mandarin fish *Siniperca scherzeri*. *J. Fish Dis.* **2018**, *41*, 1229–1233. [[CrossRef](#)] [[PubMed](#)]
35. Kwon, W.J.; Yoon, M.J.; Jin, J.W.; Kim, K.L.; Kim, Y.C.; Hong, S.; Jeong, H.D. Development and characterization of megalocytivirus persistently-infected cell cultures for high yield of virus. *Tissue and Cell* **2020**, *66*, 101387. [[CrossRef](#)]
36. Livak, K.J.; Schmittgen, T.D. Analysis of relative gene expression data using real-time quantitative PCR and the 2(-Delta Delta C(T)) Method. *Methods* **2001**, *25*, 402–408. [[CrossRef](#)]

37. Au, W.C.; Moore, P.A.; Lowther, W.; Juang, Y.T.; Pitha, P.M. Identification of a member of the interferon regulatory factor family that binds to the interferon-stimulated response element and activates expression of interferon-induced genes. *Proc. Natl. Acad. Sci. USA* **1995**, *92*, 11657–11661. [[CrossRef](#)] [[PubMed](#)]
38. Escalante, C.R.; Nistal-Villán, E.; Shen, L.; García-Sastre, A.; Aggarwal, A.K. Structure of IRF-3 bound to the PRDIII-I regulatory element of the human interferon-beta enhancer. *Mol. Cell* **2007**, *26*, 703–716. [[CrossRef](#)]
39. Xiang, Z.; Dong, C.; Qi, L.; Chen, W.; Huang, L.; Li, Z.; Xia, Q.; Liu, D.; Huang, M.; Weng, S.; et al. Characteristics of the interferon regulatory factor pairs zIFRF5/7 and their stimulation expression by ISKNV Infection in zebrafish (*Danio rerio*). *Dev. Comp. Immunol.* **2010**, *34*, 1263–1273. [[CrossRef](#)]
40. Xu, Q.Q.; Chang, M.X.; Xiao, F.S.; Huang, B.; Nie, P. The gene and virus-induced expression of IRF-5 in grass carp *Ctenopharyngodon idella*. *Vet. Immunol. Immunopathol.* **2010**, *134*, 269–278. [[CrossRef](#)]
41. Xia, J.; Hu, G.B.; Dong, X.Z.; Liu, Q.M.; Zhang, S.C. Molecular characterization and expression analysis of interferon regulatory factor 5 (IRF-5) in turbot, *Scophthalmus maximus*. *Fish Shellfish Immunol.* **2012**, *32*, 211–218. [[CrossRef](#)]
42. Liang, Y.; Liu, R.; Zhang, J.; Chen, Y.; Shan, S.; Zhu, Y.; Yang, G.; Li, H. Negative regulation of interferon regulatory factor 6 (IRF6) in interferon and NF- κ B signalling pathways of common carp (*Cyprinus carpio* L.). *BMC Vet. Res.* **2022**, *18*, 433. [[CrossRef](#)] [[PubMed](#)]
43. Meraro, D.; Hashmueli, S.; Koren, B.; Azriel, A.; Oumard, A.; Kirchoff, S.; Hauser, H.; Nagulapalli, S.; Atchison, M.L.; Levi, B.Z. Protein-protein and DNA-protein interactions affect the activity of lymphoid-specific IFN regulatory factors. *J. Immunol.* **1999**, *163*, 6468–6478. [[CrossRef](#)]
44. Yoneyama, M.; Suhara, W.; Fukuhara, Y.; Fukuda, M.; Nishida, E.; Fujita, T. Direct triggering of the type I interferon system by virus infection: Activation of a transcription factor complex containing IRF-3 and CBP/p300. *EMBO J.* **1998**, *17*, 1087–1095. [[CrossRef](#)]
45. Yang, H.; Ma, G.; Lin, C.H.; Orr, M.; Wathelet, M.G. Mechanism for transcriptional synergy between interferon regulatory factor (IRF)-3 and IRF-7 in activation of the interferon-beta gene promoter. *Eur. J. Biochem.* **2004**, *271*, 3693–3703. [[CrossRef](#)] [[PubMed](#)]
46. Marié, I.; Smith, E.; Prakash, A.; Levy, D.E. Phosphorylation-induced dimerization of interferon regulatory factor 7 unmasks DNA binding and a bipartite transactivation domain. *Mol. Cell. Biol.* **2000**, *20*, 8803–8814. [[CrossRef](#)]
47. Holland, J.W.; Bird, S.; Williamson, B.; Woudstra, C.; Mustafa, A.; Wang, T.; Zou, J.; Blaney, S.C.; Collet, B.; Secombes, C.J. Molecular characterization of IRF3 and IRF7 in rainbow trout, *Oncorhynchus mykiss*: Functional analysis and transcriptional modulation. *Mol. Immunol.* **2008**, *46*, 269–285. [[CrossRef](#)]
48. Lin, R.; Mamane, Y.; Hiscott, J. Multiple regulatory domains control IRF-7 activity in response to virus infection. *J. Biol. Chem.* **2000**, *275*, 34320–34327. [[CrossRef](#)] [[PubMed](#)]
49. Wickramaarachchi, W.D.; Wan, Q.; Lim, B.S.; Jung, H.B.; De Zoysa, M.; Park, M.A.; Lee, J.; Whang, I. Genomic characterization of interferon regulatory factor 5 from rock bream (*Oplegnathus fasciatus*) and its role in antiviral defense. *Fish Shellfish Immunol.* **2014**, *37*, 256–267. [[CrossRef](#)]
50. Zhu, Y.; Qi, C.; Shan, S.; Zhang, F.; Li, H.; An, L.; Yang, G. Characterization of common carp (*Cyprinus carpio* L.) interferon regulatory factor 5 (IRF5) and its expression in response to viral and bacterial challenges. *BMC Vet. Res.* **2016**, *12*, 127. [[CrossRef](#)]
51. Guan, Y.; Chen, X.; Luo, T.; Ao, J.; Ai, C.; Chen, X. Molecular characterization of the interferon regulatory factor (IRF) family and functional analysis of IRF11 in the large yellow croaker (*Larimichthys crocea*). *Fish Shellfish Immunol.* **2020**, *107*, 218–229. [[CrossRef](#)]
52. Yu, Y.; Wang, Q.; Huang, Z.; Ding, L.; Xu, Z. Immunoglobulins, Mucosal Immunity and Vaccination in Teleost Fish. *Front. Immunol.* **2020**, *11*, 567941. [[CrossRef](#)] [[PubMed](#)]
53. Hu, G.B.; Lou, H.M.; Dong, X.Z.; Liu, Q.M.; Zhang, S.C. Characteristics of the interferon regulatory factor 5 (IRF5) and its expression in response to LCDV and poly I:C challenges in Japanese flounder, *Paralichthys olivaceus*. *Dev. Comp. Immunol.* **2012**, *38*, 377–382. [[CrossRef](#)] [[PubMed](#)]

Disclaimer/Publisher’s Note: The statements, opinions and data contained in all publications are solely those of the individual author(s) and contributor(s) and not of MDPI and/or the editor(s). MDPI and/or the editor(s) disclaim responsibility for any injury to people or property resulting from any ideas, methods, instructions or products referred to in the content.